

## Automated, Low-Power Chamber System for Measuring Nitrous Oxide Emissions

Joel J. Fassbinder,\* Natalie M. Schultz, John M. Baker, Timothy J. Griffis

Continuous measurement of soil  $\text{N}_2\text{O}$  emissions is needed to constrain  $\text{N}_2\text{O}$  budget and emission factors. Here, we describe the performance of a low-power Teledyne  $\text{N}_2\text{O}$  analyzer and automated chamber system, powered by wind and solar, that can continuously measure soil  $\text{N}_2\text{O}$  emissions. Laboratory testing of the analyzer revealed significant temperature sensitivity, causing zero drift of  $-10.6 \text{ nmol mol}^{-1} \text{ }^\circ\text{C}^{-1}$ . However, temperature-induced span drift was negligible, so the associated error in flux measurement for a typical chamber sampling period was on the order of  $0.016 \text{ nmol m}^{-2} \text{ s}^{-2}$ . The 1-Hz precision of the analyzer over a 10-min averaging interval, after wavelet decomposition, was  $1.5 \text{ nmol mol}^{-1}$ , equal to that of a tunable diode laser  $\text{N}_2\text{O}$  analyzer. The solar/wind hybrid power system performed well during summer, but system failures increased in frequency in spring and fall, usually at night. Although increased battery storage capacity would decrease down time, supplemental power from additional sources may be needed to continuously run the system during spring and fall. The hourly flux data were numerically subsampled at weekly intervals to assess the accuracy of integrated estimates derived from manually sampling static chambers. Weekly sampling was simulated for each of the five weekdays and for various times during each day. For each weekday, the cumulative N emissions estimate using only morning measurements was similar (within 15%) to the estimate using only afternoon measurements. Often, weekly sampling partially or completely missed large episodic  $\text{N}_2\text{O}$  emissions that continuous automated chamber measurements captured, causing weekly measurements to underestimate cumulative N emissions for 9 of the 10 sampling scenarios.

AGRICULTURAL ECOSYSTEMS are the major source of nitrous oxide ( $\text{N}_2\text{O}$ ) to the atmosphere, accounting for up to 80% of anthropogenic emissions (Sehy et al., 2003) primarily due to application of N fertilizer (Maljanen et al., 2003; Parkin and Kaspar, 2006; Chirinda et al., 2010; Johnson et al., 2011). Due to an insufficient temporal and spatial representation of different field types and management practices, estimates of cumulative  $\text{N}_2\text{O}$  emissions from agricultural soils have large uncertainties, ranging from 60 to 170% of the mean estimate of  $2.8 \text{ Tg N yr}^{-1}$  (Denman et al., 2007). Accurate measurement of soil  $\text{N}_2\text{O}$  emissions remains a necessary step toward a better constraint on estimates of N loss to the atmosphere and  $\text{N}_2\text{O}$  emission factors.

Approximately 95% of soil  $\text{N}_2\text{O}$  emissions data reported in the literature have been obtained using manual static chambers (Rochette and Ericksen-Hamel, 2008). Manual chambers are commonly used (Sehy et al., 2003; Rochette and Ericksen-Hamel, 2008; Chirinda et al., 2010; Johnson et al., 2011) because they are inexpensive, have a relatively simple methodology, and require no electrical power. However, manual sampling usually provides a low temporal resolution (Parkin, 2008; Smemo et al., 2011), which can be problematic because  $\text{N}_2\text{O}$  emissions from agricultural soils are often episodic, occurring within 72 h of heavy rain when denitrifying conditions are present (Wagner-Riddle and Thurtell, 1998; Sehy et al., 2003; Johnson et al., 2011). Due to the episodic nature of soil  $\text{N}_2\text{O}$  emissions, continuous chamber measurement with high temporal resolution is preferable for budget and process studies. The use of an automated chamber system and portable  $\text{N}_2\text{O}$  gas analyzer can provide continuous measurement of  $\text{N}_2\text{O}$  emissions from agricultural soils with high temporal resolution (Parkin and Kaspar, 2006; Barton et al., 2008). Unfortunately, few agricultural study sites have on-site electrical power, which has limited the number of locations where such research can be conducted. This has created the need for low-power, portable chamber systems that can be run using electrical power produced at the site (i.e., solar, wind, gas generator, etc.). The two principal power-consuming components in an automated system are the chamber itself and the trace gas analyzer.

Copyright © American Society of Agronomy, Crop Science Society of America, and Soil Science Society of America. 5585 Guilford Rd., Madison, WI 53711 USA. All rights reserved. No part of this periodical may be reproduced or transmitted in any form or by any means, electronic or mechanical, including photocopying, recording, or any information storage and retrieval system, without permission in writing from the publisher.

J. Environ. Qual. 42:1–9 (2013)

doi:10.2134/jeq2012.0283

Received 19 July 2012.

\*Corresponding author (fass0019@umn.edu).

J.J. Fassbinder, N.M. Schultz, and J.M. Baker, USDA–ARS, Dep. of Soil, Water, and Climate, Univ. of Minnesota, 439 Borlaug Hall, 1991 Upper Buford Circle, St. Paul, MN; J.M. Baker and T.J. Griffis, Dep. of Soil, Water, and Climate, Univ. of Minnesota, 439 Borlaug Hall, 1991 Upper Buford Circle, St. Paul, MN. Assigned to Assoc. Editor Søren O. Petersen.

**Abbreviations:** DOY, day of year; GC, gas chromatography; GFC, gas filter correlation; TDL, tunable diode laser.

## Chamber Designs

Static chambers are often used to measure  $\text{N}_2\text{O}$  emissions because they are mechanically simple and because the concentration change inside of the chamber is relatively easy to detect (Denmead, 2008). Static chambers designed for  $\text{CO}_2$  and  $\text{CH}_4$  flux measurements (Raich et al., 1990; Moore and Roulet, 1991; Healy et al., 1996; Gaumont-Guay et al., 2006) are commonly used for  $\text{N}_2\text{O}$  flux measurements as well. Denmead (1979) describes an automated static chamber design for continuous measurement of soil  $\text{N}_2\text{O}$  emissions in the field. In an automated static chamber setup, sampling frequency and duration are electronically controlled. The chamber lids are mechanically closed at regular intervals, and gas from the chamber headspace is drawn to a gas analyzer and circulated back to the chamber in a closed loop by a small pump. Between measurements, the chamber lids remain in a lifted position to avoid altering the environment within the area of the chamber. Although there are a number of commercially available automatic chamber systems, it is not uncommon for researchers to design their own chamber systems. Ambus and Robertson (1998) describe an automated chamber system configured for simultaneous operation of up to 16 chambers for near-continuous measurement of  $\text{N}_2\text{O}$  and  $\text{CO}_2$ . Each chamber was constructed with a stainless steel base and a Plexiglass lid that slid closed for 1-h intervals via a linear actuator. Breuer et al. (2000) developed a highly mobile and automated chamber system using aluminum frames with acrylic glass panes that were opened and closed at regular intervals using pneumatic pistons. Recently, others have constructed automated chambers of similar designs to continuously measure soil  $\text{N}_2\text{O}$  emissions using infrared gas analyzers (e.g., Denmead et al., 2010; Jorgensen et al., 2012).

The Biometeorology and Soil Physics Group at the University of British Columbia (Gaumont-Guay et al., 2006) designed an automated chamber system consisting of large, hinged Plexiglass domes that remain open between sampling periods. These chambers were initially designed for use in forest environments but have been successfully used in agricultural fields with adjustments made to minimize wind and temperature effects (Fassbinder et al., 2012). Two commercially available automated chamber systems developed by Li-Cor (8100–101 and 8100–104, Li-Cor Inc.) for  $\text{CO}_2$  flux measurements (Madsen et al., 2009; Heinemeyer et al., 2011; Litton et al., 2011; Ruehr et al., 2012) can also be used for  $\text{N}_2\text{O}$  flux measurements in agricultural environments. Both designs move the chamber lid away from the measured soil area so that the soil inside the chamber measurement area is fully exposed, receiving normal amounts of precipitation and radiation.

## Analyzer Options

In the past, gas chromatography (GC), an analytical technique that separates a gas sample into its individual components, was the primary method for chamber-based measurements of  $\text{N}_2\text{O}$  fluxes (e.g., Mosier et al., 1991). Until recently, GC measurements of  $\text{N}_2\text{O}$  were limited to the laboratory. Gas samples manually collected from chambers via syringe were injected into evacuated vials and then transported back to the laboratory for analysis. On-site GC systems like the SRI Instruments Model 8610 can be fully automated to measure  $\text{N}_2\text{O}$  fluxes from chambers in the field

(Papen and Butterbach-Bahl, 1999; Flessa et al., 2002; Mondini et al., 2010; Wang et al., 2011). However, on-site GC systems often have a low sampling frequency (90 s) and require the use of carrier and calibration gases. In addition, GC systems typically use the radionuclide  $^{63}\text{Ni}$  in the electron capture detector cell, potentially creating bureaucratic and logistical issues.

Recent advances in spectroscopic techniques have made it possible to continuously measure  $\text{N}_2\text{O}$  under field conditions. Photoacoustic infrared detection has been widely used to measure  $\text{N}_2\text{O}$  emissions from chamber systems (Ambus and Robertson, 1998; Breuer et al., 2000; Flechard et al., 2005; Neftel et al., 2007). In photoacoustic detection, infrared light is pulsed through an appropriate optical filter before it enters the sample cell. Two microphones detect the changes in pressure caused by the gas absorption of the modulated light source, which is proportional to the concentration of the gas in the sample cell. Photoacoustic detection analyzers, such as the INNOVA Multi-Gas Analyzer (LumaSense Technologies), can simultaneously measure several greenhouse gases that absorb in infrared wavelengths. However, because many gases absorb in the infrared region, interference is a problem that requires corrections to be applied after sampling, particularly for water vapor (Flechard et al., 2005; Neftel et al., 2007).

The development of tunable diode laser (TDL) and quantum cascade laser analyzers has made high-frequency measurements (up to 10 Hz) of  $\text{N}_2\text{O}$  possible (Pihlatie et al., 2005; Mammarella et al., 2010; Neftel et al., 2010; Molodovskaya et al., 2001). In a TDL system like the TGA100A (Campbell Scientific, Inc.), a temperature- and current-controlled laser is tuned to a specific infrared absorption line of the gas of interest. The concentration is determined by passing the infrared beam through a sample cell and reference cell, and the gas concentration is proportional to the amount of energy absorbed by the gas. Tunable diode laser systems are highly precise ( $1.5 \text{ nmol mol}^{-1}$  at 10 Hz) for  $\text{N}_2\text{O}$  (Mammarella et al., 2010) but may be less desirable for remote locations because they are generally heavy (84 kg for the TGA100A), require AC power and a vacuum pump, and often require liquid nitrogen to maintain the laser at the appropriate temperature.

Gas filter correlation (GFC) analyzers may be a viable option for remote field measurement of  $\text{N}_2\text{O}$  emissions. They work by passing infrared radiation through a spinning GFC wheel before it enters the sample cell. The GFC wheel consists of two chambers: (i) a reference cell filled with a binary mixture ( $\text{N}_2$  and a high concentration of  $\text{N}_2\text{O}$ ) that is effectively opaque in the wavelengths absorbed by  $\text{N}_2\text{O}$  and (ii) a measurement cell filled with  $\text{N}_2$  that does not absorb infrared radiation. Thus, light exiting the GFC wheel into the sample cell is alternately depleted and undepleted in the  $\text{N}_2\text{O}$ -absorbing wavelengths. The intensity of radiation that reaches the photo-detector pulsates, with the amplitude of the pulse dependent on the concentration of  $\text{N}_2\text{O}$  in the sample cell. This technique allows GFC instruments to discriminate against potential interference from other gases that absorb in the same wavelengths as the gas of interest (Herget et al., 1976). Gas filter correlation analyzers like the Thermo Scientific 46i (Thermo Fisher Scientific) and the Teledyne models M320EU2 and T320U (Teledyne Instruments API) are relatively smaller and cheaper and require less maintenance than TDL systems. However, up to this point, little has been known

about the stability of these instruments in field environments. Fried and Henry (1991) conducted an intercomparison of ambient measurements of carbon monoxide using a TDL system and a GFC instrument. They found that both instruments were reliable and agreed with the standards used by each system to within 2%. To our knowledge, there have been no evaluations of the suitability of GFC  $\text{N}_2\text{O}$  analyzers for quantifying soil  $\text{N}_2\text{O}$  emissions under field conditions.

## Objectives

In this study, a gas filter correlation  $\text{N}_2\text{O}$  analyzer (Teledyne M320EU2) was combined with an automated chamber system designed for soil respiration research (Li-Cor 8100–104) to provide a low-power, portable option for continuous measurement of soil  $\text{N}_2\text{O}$  emissions. A combination of solar panels and a wind turbine provided power to the system. The objectives of this study were (i) to examine the temperature sensitivity of the Teledyne M320EU2, (ii) to compare the precision and uncertainty of the Teledyne M320EU2 with a tunable diode laser  $\text{N}_2\text{O}$  analyzer (TGA100A) for  $\text{N}_2\text{O}$  flux measurement, (iii) to describe the remote power system that was used and analyze its seasonal performance, and (iv) to use the automated chamber data to show how manual chamber sampling and time of sampling affect estimates of the  $\text{N}_2\text{O}$  budget.

## Materials and Methods

### Temperature Sensitivity Analysis

The temperature sensitivity of the Teledyne M320EU2  $\text{N}_2\text{O}$  analyzer was evaluated by placing the instrument inside a small, temperature-controlled growth chamber at the University of Minnesota St. Paul Campus. A repeating 30-min sampling sequence was established consisting of a 20-min room air sample followed by 5-min samples of two standard gases with known  $\text{N}_2\text{O}$  concentrations of  $500 \text{ nmol mol}^{-1}$  (span 1) and  $320 \text{ nmol mol}^{-1}$  (span 2), respectively. This 30-min sampling sequence was repeated throughout the experiment. The span tanks were placed outside of the enclosure in a room with a constant temperature of  $21^\circ\text{C}$ . A diel temperature cycle was set to a high temperature of  $35^\circ\text{C}$  at 1200 h and a low temperature of  $20^\circ\text{C}$  at 0000 h with gradual ramping between the two endpoints.

### Analyzer Comparison

A comparison of the Teledyne M320EU2 (gas filter correlation) and TGA100A (tunable diode laser)  $\text{N}_2\text{O}$  analyzers was performed at the University of Minnesota Rosemount Research and Outreach Center, located 25 km south of St. Paul, Minnesota. For a 15-d period, the analyzers were connected to an automated chamber system that was placed in an agricultural field 30 d after fertilizer application. The automated chamber system used for this comparison was designed by the Biometeorology and Soil Physics Group at the University of British Columbia (Gaumont-Guay et al., 2006). A detailed description of the chambers and their integration with a TDL system (e.g., TGA100A) can be found in Fassbinder et al. (2012). Briefly, two separate

subsamples of the main flow of the automated chamber system were created to bring chamber air to the TGA100A and Teledyne M3120EU2 analyzers. This arrangement allowed for nearly simultaneous sampling of chamber air. The analyzers were housed in an instrument trailer at the edge of the field that had a constant temperature of  $20^\circ\text{C}$ . The duration of each chamber sampling period was 900 s. The zero noise of the Teledyne M320EU2 and the TGA100A analyzers was obtained by calculating the standard deviation of a dataset in which each analyzer sampled zero air at 1 Hz for 900 s. This experiment was repeated using a compressed cylinder of room air instead of zero air to obtain the precision of each analyzer.

### Field Implementation of Portable Chamber System

Field research was conducted on a private agricultural field 14 km south of Northfield, Minnesota during the 2010 and 2011 corn growing seasons. The soil at the study site is a Garwin silt loam with an organic C content of 2.1%. Each spring, urea was broadcast at  $168 \text{ kg N ha}^{-1}$  before strip tillage, and an additional  $33 \text{ kg N ha}^{-1}$  was dribbled on the surface as a 28% solution at the time corn was planted.

Soil  $\text{N}_2\text{O}$  emissions were measured using an automated static chamber system. During the 2010 growing season through the 2011 spring thaw, six automated chambers were used. Shortly after corn planting in the spring of 2011 two chambers were added to the system. The chambers (LiCor Model 8100–104) use a rotary arm to open and close a chamber lid with a headspace volume of  $0.0047 \text{ m}^3$  and a cross-sectional area of  $0.03178 \text{ m}^2$ . Synflex tubing (Synflex Type 1300) carried air from inside the chamber headspace to a custom-made manifold that controlled sampling to an infrared gas analyzer (Model 840, Li-Cor Inc.) for  $\text{CO}_2$  and  $\text{H}_2\text{O}$  analyses (Fig. 1). Sample air was then passed through a column of soda lime to remove  $\text{CO}_2$  before entering the  $\text{N}_2\text{O}$  analyzer. Within the analyzer, a Nafion column removed water vapor before the sample cell. Air was pulled through the system using a diaphragm pump (Model NMP850KNDCB, KNF Neuberger Inc.), which returned the air through a manifold and back to the chamber headspace in a separate Synflex tube (return line). The flow rate through the chamber system was set at  $0.75 \text{ L min}^{-1}$ . Data collection and chamber

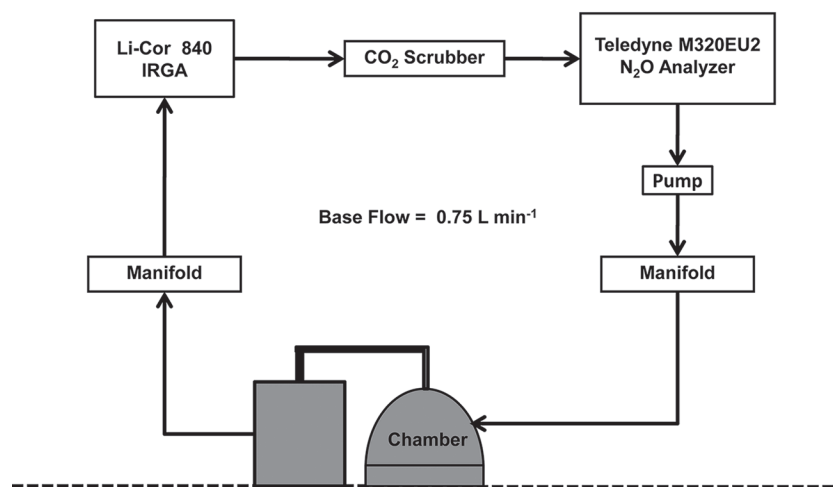


Fig. 1. Schematic of the portable chamber system used in an agricultural field near Northfield, Minnesota.



sequencing were controlled by a datalogger (CR5000, Campbell Scientific) equipped with two relay drivers (A6REL-12, Campbell Scientific) to supply power to the chambers and manifolds. Each chamber was sampled every 60 min with a sample duration time of 600 s when six chambers were installed and 450 s when eight chambers were installed.

Nitrous oxide fluxes ( $F$ ,  $\text{nmol m}^{-2} \text{s}^{-1}$ ) were calculated using Eq. [1]:

$$F = \frac{PVdC/dT}{AT_aR} \quad [1]$$

where  $P$  is atmospheric pressure (Pa),  $V$  is the geometric volume of an empty chamber ( $\text{m}^3$ ),  $dC/dt$  is the change in concentration within the chamber during a single sampling event ( $\text{nmol mol}^{-1} \text{s}^{-1}$ ),  $A$  is the surface area of the chamber ( $\text{m}^2$ ),  $T_a$  is the air temperature (K), and  $R$  is the gas constant ( $8.3144 \text{ m}^3 \text{ Pa K}^{-1} \text{ mol}^{-1}$ ). A best fit linear regression was used to determine  $dC/dt$ . To minimize nonlinearity in the  $dC/dt$  calculation, only the first 300 s of each chamber measurement were used. Dilution of the chamber  $\text{N}_2\text{O}$  concentration caused by the circulation of air to and from the chamber was not estimated. The chambers were opened at the end of each sampling period to allow the soil inside the collar to be exposed to the atmosphere. The chambers were positioned approximately 10 cm from the edge of the planted row. No vegetation was allowed to grow within the chambers. Soil collars were inserted 10 cm into the soil. The collar height was 5 cm above the ground, minimizing the reduction of air flow over the collared soil (Jassal et al., 2012).

## Power Production System

A wind turbine (Whisper Wind Generator, Model 200, Southwest Windpower) and four 130 W solar panels (Model KD130GX-LPU, Kyocera Solar Inc.) were used to charge 11 DC deep cycle 12 V batteries (Fig. 2) at the Northfield, Minnesota field site. A DC-to-AC inverter (PowerVerter Model PV700HF, Tripp Lite) provided AC power that was carried to a small instrument shelter in the field where the analyzers and datalogger were housed. Only the  $\text{N}_2\text{O}$  analyzer used AC power. The datalogger, chambers, and  $\text{CO}_2/\text{H}_2\text{O}$  gas analyzer used DC power. When the battery voltage dropped below 10.5 V DC, power to the entire system was automatically turned off to allow the solar panels and wind turbine to fully charge the battery bank. Power was restored when the voltage of the battery bank reached 13 V DC. The total continuous power requirement for the system was about 350 W at startup, the majority of which was used by the internal heater of the  $\text{N}_2\text{O}$  analyzer. Once the operating temperature of the analyzer was reached, the system required about 150 W of continuous power.

## Effect of Manual Chamber Sampling on Cumulative Nitrogen Emissions

The traditional method of manual chamber sampling may not accurately capture soil  $\text{N}_2\text{O}$  emissions, which often occur in relatively short, episodic events. Manual static chambers are typically measured at a low temporal resolution (weekly to semi-weekly) (Parkin, 2008), likely missing episodic emissions and thus

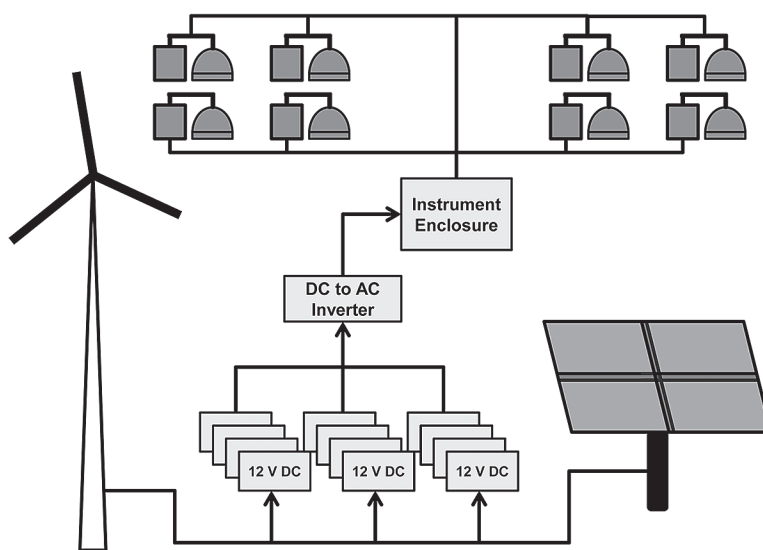


Fig. 2. Schematic of the power system for remote operation of automated chambers in an agricultural field near Northfield, Minnesota.

resulting in inaccurate annual  $\text{N}_2\text{O}$  budgets. To investigate the effect of manual chamber sampling on cumulative N emissions, the automated chamber data were numerically subsampled to simulate a weekly sampling schedule. Weekly subsamples were divided into morning-only (0900–1100 h) and afternoon-only (1400–1600 h) scenarios. Weekly simulated sampling was performed on each of the five weekdays (Monday–Friday), creating morning and afternoon cumulative N emissions for each weekday. No measurements that fell on the weekend (Saturday and Sunday) were included in the analysis. For each scenario, flux measurements from all of the chambers were averaged to obtain a mean emission rate. Cumulative estimates of N emissions for each of the five weekdays were obtained from the integration of the mean emission rates (Smith and Dobbie, 2001; Parkin, 2008).

## Results and Discussion

### Temperature Sensitivity of the Teledyne M320EU2

Temperature-induced drift of the Teledyne M320EU2 was quantified to determine its potential influence on chamber  $\text{N}_2\text{O}$  flux measurements. When the instrument was exposed to a diel temperature cycle of 20 to 35°C, drift was significant. As the temperature increased from 20 to 35°C, the apparent concentrations of span 1 and span 2 decreased from 490 and 320  $\text{nmol mol}^{-1}$  to 330 and 160  $\text{nmol mol}^{-1}$ , respectively (Fig. 3). Across the entire temperature range, however, the difference between the span tanks was consistently about 170  $\text{nmol mol}^{-1}$ , indicating that the temperature response was a zero drift rather than a span drift. The zero drift was approximately linear, with a slope of  $-10.6 \text{ nmol mol}^{-1} \text{ } ^\circ\text{C}^{-1}$  ( $r^2 = 0.95$ ). Routine calibration (every 30 min) using the two span gases eliminated the temperature-induced drift (not shown).

The temperature sensitivity of the Teledyne M320EU2 was tested at the agricultural field in Northfield, Minnesota by sampling a reference gas (320  $\text{nmol mol}^{-1}$ ) for 300 s every 60 min while a thermocouple continuously measured the diel temperature change inside of the enclosure that housed the analyzer. Field testing during the growing season revealed a similar temperature sensitivity to what was exhibited in the

laboratory ( $-9.1 \text{ nmol mol}^{-1} \text{ }^{\circ}\text{C}^{-1}$ ;  $r^2 = 0.95$ ). During the summer, the temperature inside the instrument enclosure often exceeded  $35^{\circ}\text{C}$  in the afternoon, with nighttime lows near  $20^{\circ}\text{C}$ . Although the temperature sensitivity of the Teledyne M320EU2 is a concern, thermal inertia of the unit is sufficiently large that the drift is only about  $3 \text{ nmol mol}^{-1}$  during a 10-min chamber sample, which alters the flux measurement by only  $0.016 \text{ nmol m}^{-2} \text{ s}^{-1}$ . The flux can be corrected using the known sensitivity of the Teledyne M320EU2 and the measured temperature of the instrument enclosure.

### Comparison of the Teledyne M320EU2 and TGA100A Nitrous Oxide Analyzers

The zero noise and precision values of the Teledyne M320EU2 and TGA100A were quantified to determine uncertainty in the flux measurement. The zero noise of the unfiltered Teledyne M320EU2 output was  $7.5 \text{ nmol mol}^{-1}$  for a 15-min chamber sample, compared with  $1.6 \text{ nmol mol}^{-1}$  for the TGA100A. A noise reduction technique based on wavelet decomposition (Wavelet Toolbox, Matlab, Version R2010bSP1, Mathworks) was applied to the Teledyne M320EU2 output, which reduced the zero noise to  $1.8 \text{ nmol mol}^{-1}$ . When sampling compressed cylinder air, precision values were  $8.1 \text{ nmol mol}^{-1}$  for the unfiltered Teledyne M320EU2 output,  $1.5 \text{ nmol mol}^{-1}$

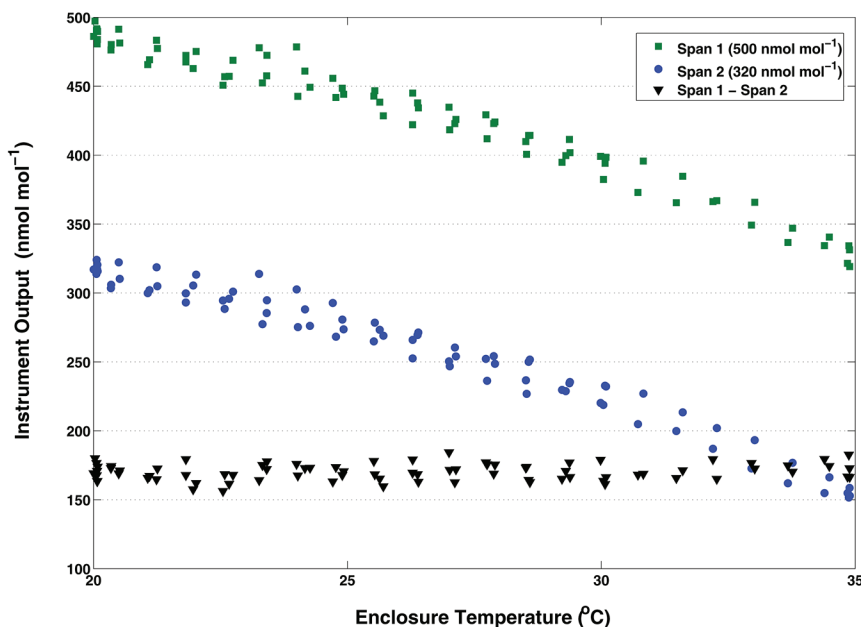


Fig. 3. Temperature sensitivity of the Teledyne M320EU2  $\text{N}_2\text{O}$  analyzer showing mean instrument output while measuring a  $500 \text{ nmol mol}^{-1}$  span tank (green squares) and a  $320 \text{ nmol mol}^{-1}$  span tank (blue circles). The black triangles represent the difference between the two span tanks.

for the Teledyne M320EU2 output with noise reduction, and  $1.5 \text{ nmol mol}^{-1}$  for the TGA100A. These precision values were used as the  $dC$  term in Eq. [1] to obtain the minimum detectable flux, which was calculated as  $0.16 \text{ nmol m}^{-2} \text{ s}^{-1}$  for the unfiltered Teledyne M320EU2 output,  $0.028 \text{ nmol m}^{-2} \text{ s}^{-1}$  when noise reduction was applied, and  $0.028 \text{ nmol m}^{-2} \text{ s}^{-1}$  for the TGA100A. For the unfiltered Teledyne M320EU2 output, the typical standard deviation of  $dC/dt$  for a 15-min chamber sample

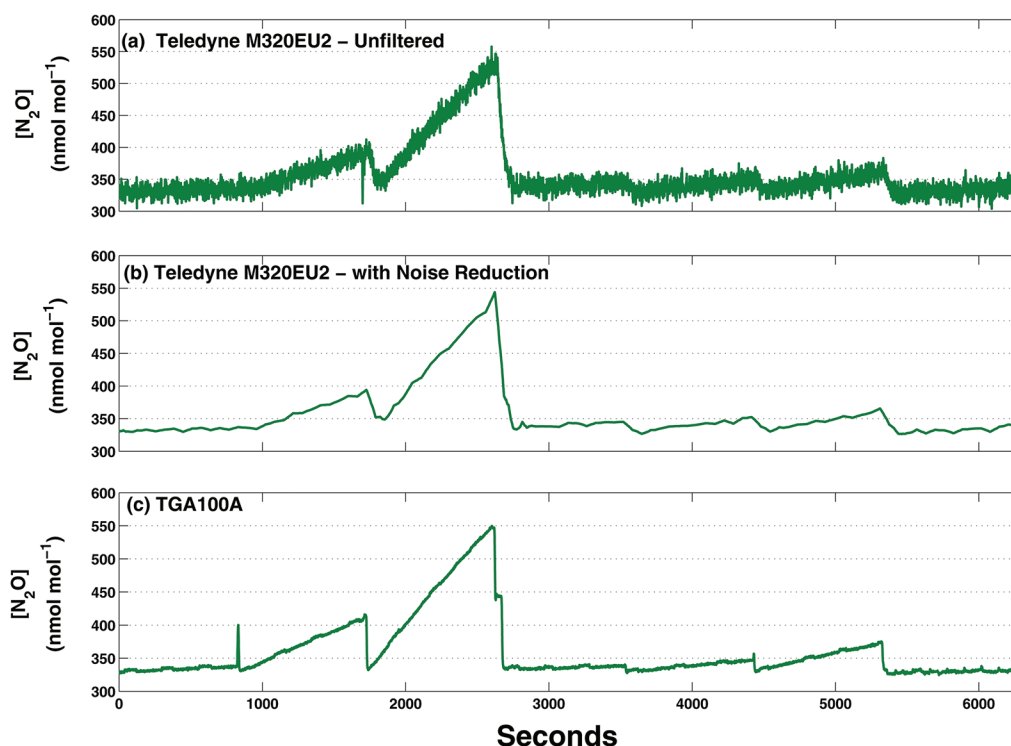


Fig. 4. Nitrous oxide analyzer comparison showing raw data of seven chamber measurements from the (a) Teledyne M320EU2 (unfiltered), (b) Teledyne M320EU2 (with noise reduction), and (c) TGA100A.

was  $0.003 \text{ nmol s}^{-1}$ , resulting in a flux uncertainty of  $0.02 \text{ nmol m}^{-2} \text{ s}^{-1}$ . When noise reduction was applied, the typical standard deviation of  $dC/dt$  was  $0.0005 \text{ nmol s}^{-1}$ , which decreased the flux uncertainty to  $0.003 \text{ nmol m}^{-2} \text{ s}^{-1}$ . The typical standard deviation of  $dC/dt$  for the TGA100A was  $0.0003 \text{ nmol s}^{-1}$ , which resulted in a flux uncertainty of  $0.002 \text{ nmol m}^{-2} \text{ s}^{-1}$ . Further comparison of the Teledyne M320EU2 and TGA100A was performed by connecting both analyzers to an automated chamber system for 15 d. A portion of raw data (6300 s) from these chamber measurements is shown in Fig. 4. Comparison of the Teledyne-measured fluxes against those measured with the TGA100A is shown in Fig. 5. Noise reduction was applied to the unfiltered Teledyne M320EU2 data for this flux measurement comparison. The scatter about the 1:1 line is relatively minor, although there is possible evidence of bias at the highest fluxes.

## Power System for Remote Operation of Portable Chambers

In early spring, inconsistent wind speed and cloud cover often led to inadequate power production and system failure (Fig. 6). An example of the inconsistent nature of spring power production occurred in late March of 2012 (day of year [DOY] 78–88). From DOY 78 to 80, strong wind ( $>4 \text{ ms}^{-1}$ ) provided enough power to operate the chamber system despite heavy cloud cover. Over the next 48 h, power production was poor due to calm, cloudy conditions, which led to system failure on DOY 82. Light cloud cover from DOY 83 to 84 allowed the solar panels to recharge the battery bank, and the chamber system was restarted on DOY 84. After a brief power failure during the early morning of DOY 85, strong winds allowed the chamber system to operate despite mostly cloudy conditions.

The power system was most effective during the late spring through the late summer. Although the average wind speed is relatively low during this period ( $<2 \text{ ms}^{-1}$ ), daytime insolation often exceeds  $800 \text{ W m}^{-2}$ , which allows the chamber system to operate solely on solar power. In addition, warmer air temperatures during the summertime decrease the power required to maintain the Teledyne M320EU2 operating temperature.

In 2010, 13.7% of potential chamber measurements were lost during the 147-d sampling campaign due to an inadequate supply of power. Increased battery storage capacity and an additional solar panel decreased this percentage to 11.1 during the 127-d sampling campaign

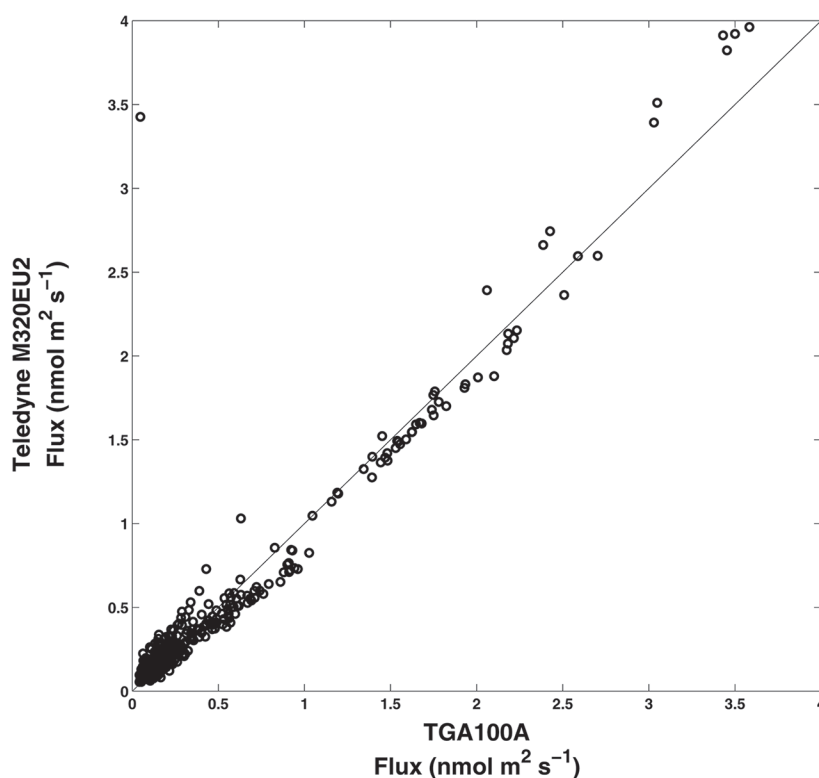


Fig. 5. A one-to-one comparison of  $\text{N}_2\text{O}$  chamber flux measurements from the TGA100A and Teledyne M320EU2 analyzers.

in 2011. A major challenge for the solar/wind power system is to provide enough battery power for nighttime operation of the chamber system. In total, 84% (21/25) of chamber system failures that were caused by an inadequate supply of power occurred between 0300 and 0700 h. Because daytime power production often exceeds power consumption during the late

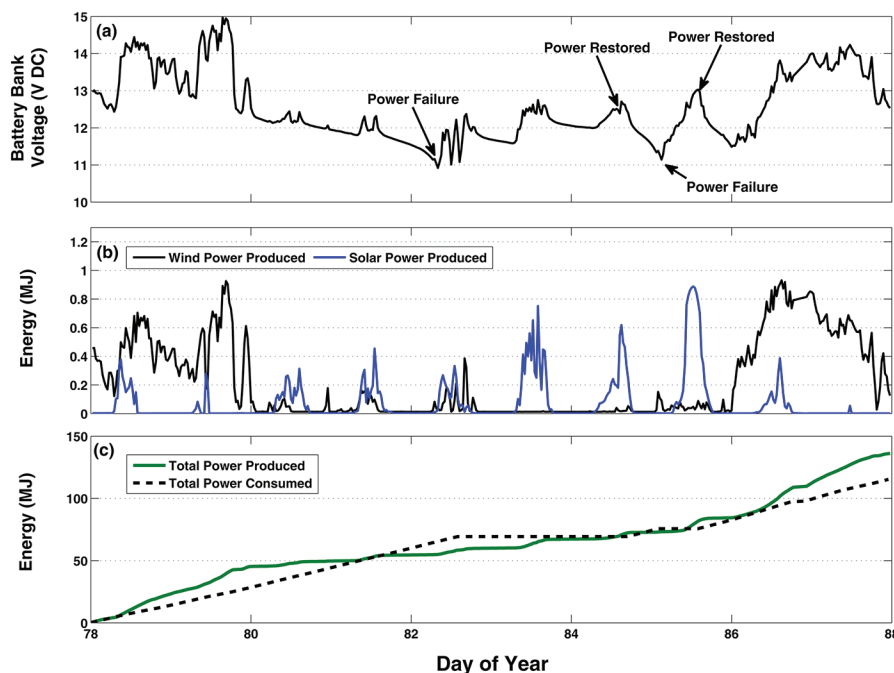


Fig. 6. Half-hourly measurements of (a) battery bank voltage, (b) power production from the wind turbine (black line) and solar panels (blue line), and (c) cumulative sums of total power production (green line) and power consumption by the automated chamber system (black dashes). Measurements were taken for a 10-d period during the spring of 2012.

spring to late summer, additional battery storage capacity should decrease system failures and allow the chamber system to operate through the early morning. In the early spring and late fall, inadequate daytime power production may also contribute to system failure. Under calm conditions, powering of the chamber system overnight lowers the voltage of the battery bank by up to 2 V DC during these periods. Yang et al. (2008) found that a battery bank with 3 to 5 d of storage capacity is suitable for a small solar/wind hybrid power production system. The battery bank used for our system (11 DC deep cycle 12 V batteries) can provide 1100 Ah of power when fully charged, corresponding to approximately 2.0 to 3.5 d of storage capacity for the chamber system. To provide 5 d of storage capacity for the chamber system, our battery bank would need an additional four batteries in the summer and an additional 16 batteries in the spring and fall. Considering the challenge of hauling batteries to remote sites, the best strategy might be adding four batteries to accommodate production during the summer and a secondary power source (i.e., gas generator) during the spring and fall.

### Sampling Frequency and Cumulative Nitrogen Emissions

The automated chamber flux measurements were numerically subsampled to simulate weekly manual sampling. Weekly subsampling was conducted for each of the five weekdays (Monday–Friday) and included morning-only and afternoon-only sampling scenarios, creating 10 subsamples that were integrated to produce cumulative N emissions for the growing season. Mean hourly emission rates from the 2010 corn growing season were used for the analysis and are shown in Fig. 7. In 2010, automated chamber sampling was performed from DOY 135 to 282 (15 May to 9 Oct.). Emissions were greatest 20 to 50 d after fertilizer application from DOY 140 to 160, with mean hourly rates reaching  $3.3 \text{ nmol m}^{-2} \text{ s}^{-1}$ . During this period, the typical standard deviation of the mean hourly emission rate was  $0.7 \text{ nmol m}^{-2} \text{ s}^{-1}$ . From about DOY 180 to 260 (29 June to 17 Sept.),  $\text{N}_2\text{O}$  emissions were near zero, with occasional episodic fluxes of up to  $0.4 \text{ nmol m}^{-2} \text{ s}^{-1}$  observed shortly after rain events. The typical standard deviation of the mean hourly emission rate during this period was  $0.05 \text{ nmol m}^{-2} \text{ s}^{-1}$ . On DOY 266 (23 Sept.), a heavy rain event (21 cm) caused a rapid increase in  $\text{N}_2\text{O}$  emissions. The episodic event lasted for about 24 h after the rain,

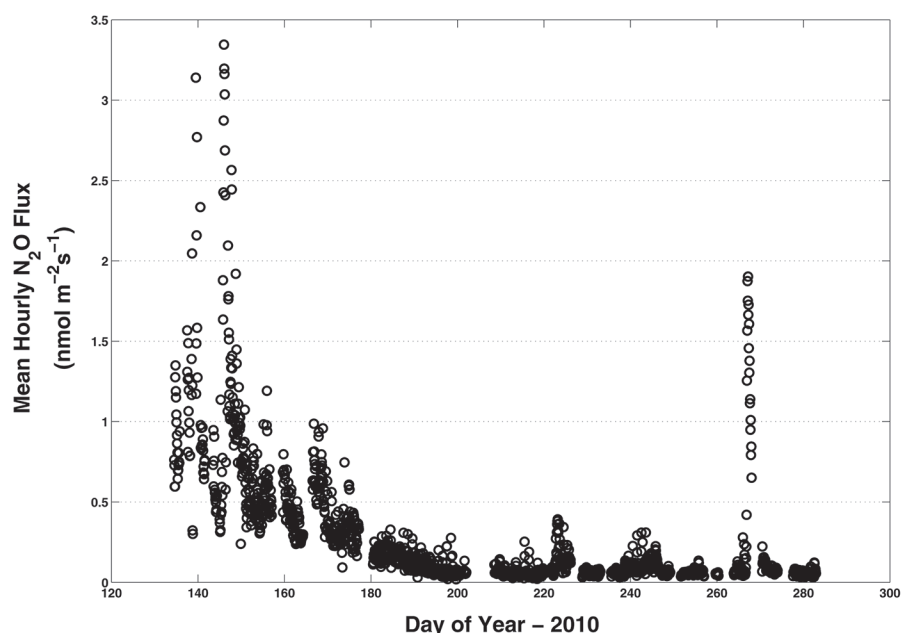


Fig. 7. Mean hourly  $\text{N}_2\text{O}$  flux measured by an automated chamber system at a private field near Northfield, Minnesota during the 2010 corn growing season.

and the mean hourly emission rate reached  $1.9 \text{ nmol m}^{-2} \text{ s}^{-1}$ . Using the hourly mean chamber data, cumulative N loss was estimated at  $102.7 \text{ mg N m}^{-2}$  for the 2010 growing season (Fig. 8a and 8b).

Cumulative estimates using the weekly morning measurement scenario were lower than the hourly mean estimate for four of the five weekdays, with totals ranging from  $66.4 \text{ mg N m}^{-2}$  (Thursday) to  $113.9 \text{ mg N m}^{-2}$  (Tuesday) (Fig. 8a). On average, the morning-only scenario underestimated the cumulative N emissions by 15.4% when compared with the hourly mean estimate, similar to the 14.3% underestimation observed by Parkin (2008). For the afternoon-only sampling scenario, all

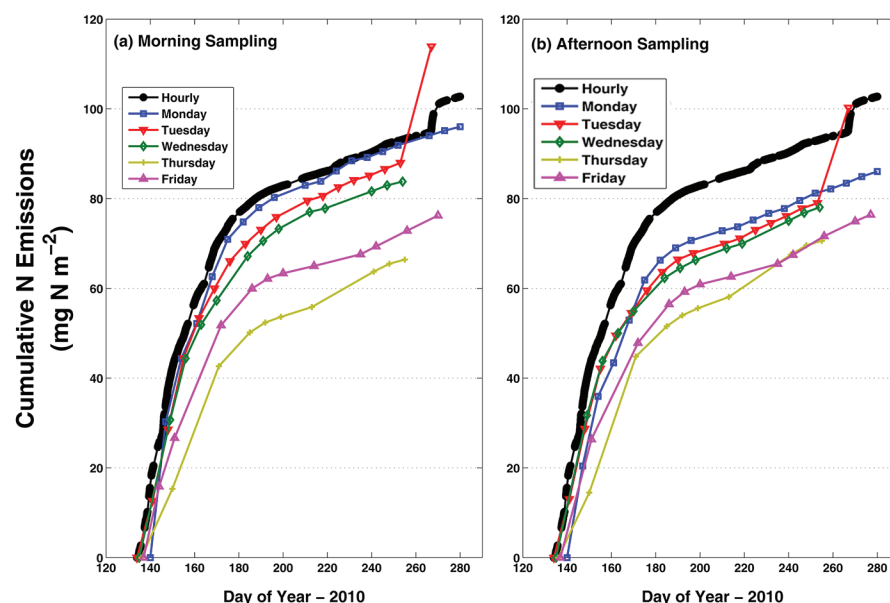


Fig. 8. Estimates of cumulative N emissions for the 2010 growing season using only (a) morning samples and (b) afternoon samples at an agricultural field near Northfield, Minnesota. Chamber measurements were numerically sampled at a weekly frequency for each of the five weekdays (Monday–Friday).



five weekdays produced cumulative N emissions that were lower than the mean hourly estimate (Fig. 8b), ranging from 70.6 mg N m<sup>-2</sup> (Thursday) to 100.3 mg N m<sup>-2</sup> (Tuesday). The average estimate of cumulative N emissions for the afternoon-only scenario was 21% lower than the hourly mean estimate. This underestimation contrasts with that of Parkin (2008), who found that the influence from daily temperature change on soil N<sub>2</sub>O emissions led to a 4.6 to 12.9% overestimation when using afternoon measurements. Unlike Parkin (2008), our study found little correlation between N<sub>2</sub>O emissions and the diel temperature pattern except for a 72-h period early in the growing season shortly after fertilizer application. Instead, flux episodes appeared to be more influenced by the timing and intensity of rain events. Without a consistent diel pattern in N<sub>2</sub>O emissions, cumulative estimates for the morning-only and afternoon-only scenarios were similar to one another (within 15%) for each of the five weekdays. Because simulated manual sampling was confined to the working hours of five weekdays, episodic N<sub>2</sub>O emissions captured by continuous automated chamber measurement were often partially or completely missed, causing 9 of the 10 weekly subsamples to produce cumulative estimates that were lower than the hourly mean estimate. Only automated chamber measurements that fell on a Tuesday morning produced a cumulative estimate that was greater than the hourly mean estimate. The cumulative estimates for the Tuesday morning and Tuesday afternoon sampling scenarios increased sharply on DOY 267 due to episodic N<sub>2</sub>O emissions caused by a 21-cm rain event on DOY 266. Because this emissions episode occurred from 0100 h Tuesday morning until 2200 h Tuesday night, none of the other four weekdays was affected.

## Conclusions and Recommendations

The combination of the Teledyne N<sub>2</sub>O analyzer and the Licor chamber system with a power generation and storage system allowed for automated measurement of soil N<sub>2</sub>O emissions in a remote field setting. When noise reduction was applied to the raw data of the Teledyne M320EU2, the analyzer precision and the uncertainty in the flux measurement improved by an order of magnitude, yielding acceptable agreement with a tunable diode laser analyzer. Also, noise reduction significantly lowered the minimum detectable flux of the analyzer, allowing for application in field settings where N<sub>2</sub>O emissions are low (<0.5 nmol m<sup>-2</sup> s<sup>-1</sup>). Although temperature-induced zero drift of the Teledyne M320EU2 is significant, the span drift is negligible, so the impact on flux measurements is trivial. Analysis of the power consumption at our field site shows that increased battery storage capacity would likely decrease the number of system failures. However, during the spring and fall supplemental power from alternative sources may be required for continuous operation of the chamber system. Numerical subsampling of the hourly automated chamber measurements showed that the morning-only and afternoon-only sampling scenarios produced similar cumulative N emissions estimates for each of the five weekdays. In addition, weekly manual sampling partially or missed episodic N<sub>2</sub>O emissions that continuous automated chamber measurements were able to capture, causing manual measurements to underestimate cumulative N emissions for 9 of the 10 sampling scenarios.

## Acknowledgments

The authors thank Matt Erickson and Bill Breiter for technical assistance at the field site and laboratory. Funding for this research was provided by the U.S. Department of Agriculture, NIFA/2010-65112-20528, and the U.S. Department of Energy through the Sun Grant Initiative (58-3625-8-478).

## References

- Ambus, P., and G. Robertson. 1998. Automated near-continuous measurement of carbon dioxide and nitrous oxide fluxes from soil. *Soil Sci. Soc. Am. J.* 62:394–400. doi:10.2136/sssaj1998.03615995006200020015x
- Barton, R., D. Gatter, K. Butterbach-Bahl, R. Buck, C. Hinz, and D. Murphy. 2008. Nitrous oxide emissions from a cropped soil in a semi-arid climate. *Glob. Change Biol.* 14:177–192.
- Breuer, L., H. Papen, and K. Butterbach-Bahl. 2000. N<sub>2</sub>O emission from tropical forest soils of Australia. *J. Geophys. Res.* 105:26353–26367.
- Chirinda, N., M.S. Carter, K.R. Albert, P. Ambus, J.E. Olesen, J.R. Porter, and S.O. Petersen. 2010. Emissions of nitrous oxide from arable organic and conventional cropping systems on two soil types. *Agric. Ecosyst. Environ.* 136:199–208. doi:10.1016/j.agee.2009.11.012
- Denman, K.L., G. Brasseur, A. Chidthaisong, R. Ciais, P.M. Cox, R.E. Dickinson, D. Hauglustaine, C. Heinze, E. Holland, D. Jacob, U. Lohmann, S. Ramachandran, P.L. da Silva Dias, S.C. Wofsy, and X. Zhang. 2007. Couplings between changes in the climate system and biogeochemistry. In: S. Solomon et al., editors, *Climate change 2007: The physical science basis. Contribution of Working Group I to the Fourth Assessment Report of the Intergovernmental Panel on Climate Change*. Cambridge Univ. Press, New York. p. 499–587.
- Denmead, O. 1979. Chamber systems for measuring nitrous oxide emission from soils in the field. *Soil Sci. Soc. Am. J.* 43:89–95.
- Denmead, O. 2008. Approaches to measuring fluxes of methane and nitrous oxide between landscapes and the atmosphere. *Plant Soil* 309:5–24. doi:10.1007/s11104-008-9599-z
- Denmead, O., B. Macdonald, G. Bryant, T. Naylor, S. Wilson, D. Griffith, W. Wang, B. Salter, I. White, and P. Moody. 2010. Emissions of methane and nitrous oxide from Australian sugarcane soils. *Agric. For. Meteorol.* 150:748–756. doi:10.1016/j.agrformet.2009.06.018
- Fassbinder, J., T. Griffis, and J. Baker. 2012. Interannual, seasonal, and diel variability in the carbon isotope composition of respiration in a C3/C4 agricultural ecosystem. *Agric. For. Meteorol.* 153:144–153.
- Flechar, C., A. Neff, M. Jocher, C. Amman, and J. Fuhrer. 2005. Bi-directional soil/atmosphere N<sub>2</sub>O exchange over two mown grassland systems with contrasting management practices. *Glob. Change Biol.* 11:2114–2127. doi:10.1111/j.1365-2486.2005.01056.x
- Flessa, H., R. Ruser, R. Schilling, N. Löffel, J.C. Munich, E.A. Kaiser, and F. Beese. 2002. N<sub>2</sub>O and CH<sub>4</sub> fluxes in potato fields: Automated measurement, management effects and temporal variation. *Geoderma* 105:307–325. doi:10.1016/S0016-7061(01)00110-0
- Fried, A., and B. Henry. 1991. Intercomparison of tunable diode laser and gas filter correlation measurements of ambient carbon monoxide. *Atmos. Environ.* 25A:2277–2284.
- Gaumont-Guay, D., T. Black, A. Barr, R. Jassal, and Z. Nescic. 2006. Interpreting the dependence of soil respiration on soil temperature and water content in a boreal aspen stand. *Agric. For. Meteorol.* 140:220–235. doi:10.1016/j.agrformet.2006.08.003
- Healy, R.W., R.G. Striegl, T.F. Russell, G.L. Hutchinson, and G.P. Livingston. 1996. Numerical evaluation of static-chamber measurements of soil-atmosphere gas exchange: Identification of physical processes. *Soil Sci. Soc. Am. J.* 60:740–747.
- Heinemeyer, A., C. Di Bene, A.R. Lloyd, D. Tortorella, R. Baxter, B. Huntley, A. Gelsomino, and P. Ineson. 2011. Soil respiration: Implications of the plant-soil continuum and respiration chamber collar-insertion depth on measurement and modeling of soil CO<sub>2</sub> efflux rates in three ecosystems. *Eur. J. Soil Sci.* 62:82–94. doi:10.1111/j.1365-2389.2010.01331.x
- Herget, W., J. Jahnke, D. Burch, and D. Gryvnak. 1976. Infrared gas-filter correlation instrument for in situ measurement of gaseous pollutant concentrations. *Appl. Opt.* 15:1222–1228. doi:10.1364/AO.15.001222
- Jassal, R., T. Black, Z. Nescic, and D. Gaumont-Guay. 2012. Using automated non-steady-state chamber systems for making continuous long-term measurements of soil CO<sub>2</sub> efflux in forest ecosystems. *Agric. For. Meteorol.* 161:57–65. doi:10.1016/j.agrformet.2012.03.009
- Johnson, J., D. Archer, S. Weyers, and N. Barbour. 2011. Do mitigation strategies reduce global warming potential in the northern U.S. corn belt? *J. Environ. Qual.* 40:1551–1559. doi:10.2134/jeq2011.0105



- Jorgensen, C., S. Struwe, and B. Elbering. 2012. Temporal trends in N<sub>2</sub>O flux dynamics in a Danish wetland- effects of plant-mediated gas transport of N<sub>2</sub>O and O<sub>2</sub> following changes in water level and soil mineral-N availability. *Glob. Change Biol.* 18:210–222. doi:10.1111/j.1365-2486.2011.02485.x
- Litton, C.M., C.P. Giardina, J.K. Albano, M.S. Long, and G.P. Asner. 2011. The magnitude and variability of soil-surface CO<sub>2</sub> efflux increase with mean annual temperature in Hawaiian tropical montane wet forests. *Soil Biol. Biochem.* 43:2315–2323. doi:10.1016/j.soilbio.2011.08.004
- Madsen, R., L. Xu, B. Claassen, and D. McDermitt. 2009. Surface monitoring method for carbon capture and storage projects. *Energy Procedia* 1:2161–2168. doi:10.1016/j.egypro.2009.01.281
- Maljanen, M., A. Liikanen, J. Silvola, and P. Martikainen. 2003. Measuring N<sub>2</sub>O emissions from organic soils by closed chamber or soil/snow N<sub>2</sub>O gradient methods. *Eur. J. Soil Sci.* 54:625–631. doi:10.1046/j.1365-2389.2003.00531.x
- Mammarella, I., P. Werle, M. Pihlatie, W. Eugster, S. Haapanala, R. Kiese, T. Markkanen, U. Rannik, and T. Vesala. 2010. A case study of eddy covariance flux of N<sub>2</sub>O measured within forest ecosystems: Quality control and flux error analysis. *Biogeosciences* 7:427–440. doi:10.5194/bg-7-427-2010
- Molodovskaya, M., J. Warland, B. Richards, G. Oberg, and T. Steenhuis. 2001. Nitrous oxide from heterogeneous agricultural landscapes: Source contribution analysis by eddy covariance and chambers. *Soil Sci. Soc. Am. J.* 75:1829–1838.
- Mondini, C., T. Sinicco, M. Cayuela, and M. Sanchez-Monedero. 2010. A simple automated system for measuring soil respiration by gas chromatography. *Talanta* 81:849–855. doi:10.1016/j.talanta.2010.01.026
- Moore, T.R., and N.T. Roulet. 1991. A comparison of dynamic and static chambers for methane emission measurements from subarctic fens. *Atmos.-ocean* 29:102–109. doi:10.1080/07055900.1991.9649395
- Mosier, A., D. Schimel, D. Valentine, K. Bronson, and W. Parton. 1991. Methane and nitrous oxide fluxes in native, fertilized and cultivated grasslands. *Nature* 350:330–332. doi:10.1038/350330a0
- Neffel, A., C. Ammann, C. Fischer, C. Spirig, F. Conen, L. Emmenegger, B. Tuzson, and S. Wahlen. 2010. N<sub>2</sub>O exchange over managed grassland: Application of a quantum cascade laser spectrometer for micrometeorological flux measurements. *Agric. For. Meteorol.* 150:775–785. doi:10.1016/j.agrformet.2009.07.013
- Neffel, A., C. Flechard, C. Ammann, F. Conen, L. Emmenegger, and K. Zeyer. 2007. Experimental assessment of N<sub>2</sub>O background fluxes in grassland systems. *Tellus* 59B:470–482.
- Papen, H., and K. Butterbach-Bahl. 1999. A 3-year continuous record of nitrogen trace gas fluxes from untreated and limed soil of a N-saturated spruce and beech forest ecosystem in Germany: 1. N<sub>2</sub>O emissions. *J. Geophys. Res. Atmos.* 104:18487–18503. doi:10.1029/1999JD900293
- Parkin, T. 2008. Effect of sampling frequency on estimates of cumulative nitrous oxide emissions. *J. Environ. Qual.* 37:1390–1395. doi:10.2134/jeq2007.0333
- Parkin, T., and T. Kaspar. 2006. Nitrous oxide emissions from corn-soybean systems in the Midwest. *J. Environ. Qual.* 35:1496–1506. doi:10.2134/jeq2005.0183
- Pihlatie, M., J. Rinne, P. Ambus, K. Pilegaard, J. Dorsey, U. Rannik, T. Markkanen, S. Launiainen, and T. Vesala. 2005. Nitrous oxide emissions from a beech forest floor measured by eddy covariance and soil enclosure techniques. *Biogeosciences* 2:377–387. doi:10.5194/bg-2-377-2005
- Raich, J.W., R.D. Bowden, and P.A. Steudler. 1990. Comparison of two static chamber techniques for determining carbon dioxide efflux from forest soils. *Soil Sci. Soc. Am. J.* 54:1754–1757.
- Ruehr, N.K., J.G. Martin, and B.E. Law. 2012. Effects of water availability on carbon and water exchange in a young ponderosa pine forest: Above- and belowground responses. *Agric. For. Meteorol.* 164:136–148. doi:10.1016/j.agrformet.2012.05.015
- Rochette, P., and N. Eriksen-Hamel. 2008. Chamber measurements of soil nitrous oxide flux: Are absolute values reliable? *Soil Sci. Soc. Am. J.* 72:331–342.
- Sehy, U., R. Ruser, and J. Munch. 2003. Nitrous oxide fluxes from maize fields: Relationship to yield, site-specific fertilization, and soil conditions. *Agric. Ecosyst. Environ.* 99:97–111. doi:10.1016/S0167-8809(03)00139-7
- Smemo, K., N. Ostrom, M. Opdyke, P. Ostrom, S. Bohm, and G. Robertson. 2011. Improving process-based estimates of N<sub>2</sub>O emissions from soil using temporally extensive chamber techniques and stable isotopes. *Nutr. Cycling Agroecosyst.* 91:145–154. doi:10.1007/s10705-011-9452-2
- Smith, K., and K. Dobbie. 2001. The impact of sampling frequency and sampling times on chamber-based measurements of N<sub>2</sub>O emissions from fertilized soils. *Glob. Change Biol.* 7:933–945. doi:10.1046/j.1354-1013.2001.00450.x
- Wagner-Riddle, C., and G. Thurtell. 1998. Nitrous oxide emissions from agricultural fields during winter and spring thaw as affected by management practices. *Nutr. Cycling Agroecosyst.* 52:151–163. doi:10.1023/A:1009788411566
- Wang, W., R. Dalal, S. Reeves, K. Butterbach-Bahl, and R. Kiese. 2011. Greenhouse gas fluxes from an Australian subtropical cropland under long-term contrasting management regimes. *Glob. Change Biol.* 17:3089–3101. doi:10.1111/j.1365-2486.2011.02458.x
- Yang, H., W. Zhou, L. Lu, and Z. Fang. 2008. Optimal sizing method for stand-alone hybrid solarwind system with LPSP technology by using genetic algorithm. *Sol. Energy* 82:354–367. doi:10.1016/j.solener.2007.08.005